3-D ANALYSIS OF A HIGH DENSITY BRUSH WITH FRICTIONAL CONTACT INTERACTIONS

Mahmut F. Aksit*
Sabanci University, Istanbul, Turkey, 34956

ABSTRACT

The physical complexity of dense brush structures presents major challenges to analyzers. As they maintain their flexibility at elevated temperatures, which are typical in gas turbines, high density brush seals made of super-alloy bristles found popularity among engine designers. Typically brush-rotor contact occurs at very high surface speeds. If not managed properly, this may result in extreme wear conditions and damage to rotor. In order to ensure engine operational safety brush contact loads should be controlled through seal design and detail analysis. In addition to the physical complexity of these dense brush structures, frictional contacts among the bristles themselves, between the bristles and the support plates, and between the bristles tips and the high speed rotor further increase the analysis complexity, and make it a major undertaking if not impossible. Detailed understanding of brush seal contact loads is necessary to estimate seal and rotor wear performance. The complicated nature of bristle behavior under various combinations of pressure load and rotor interference requires computer analysis to study details that may not be available through analytical formulations. This work presents a 3-D computational brush seal structural FE model that can be used to calculate bristle stress, tip force, and do wear analysis. The analysis includes a representative brush segment with bristles formed by 3-D beam elements. Bristle interlocking and frictional interactions (interbristle, bristle-backing plate and bristle-rotor) are included to better simulate pressure-stiffness coupling. Various analysis results are presented and compared to full scale seal wear tests.

INTRODUCTION

The brush seal consists of a set of fine diameter fibers densely packed between retaining and backing plates. As illustrated in Fig. 1, the backing plate is positioned downstream of the bristles to provide mechanical support under differential pressure loads. The bristles touch the rotor with a lay angle in the direction of the rotor rotation allowing them to bend rather than buckle during rotor excursions. Last few decades, brush seals have been extensively used in secondary flow sealing in turbo-machinery applications. They have demonstrated excellent leakage characteristics.

Differential pressure across a seal pushes the bristles against the backing plate. Due to mechanical interlocking as well as the frictional mechanisms, bristles stick to one another. The bristle pack also sticks to the backing plate. The frictional resistance at the backing plate causes a large increase in the contact loads at the rotor surface. When subjected to a radial interference under a sealing pressure, the seal feels much stiffer than it does without any pressure load. This leads to increased wear rates which reduce the seal life.

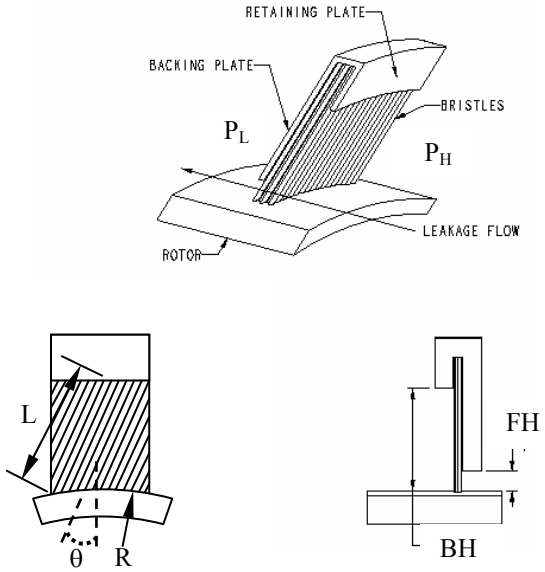

Fig. 1 Brush seal geometry.

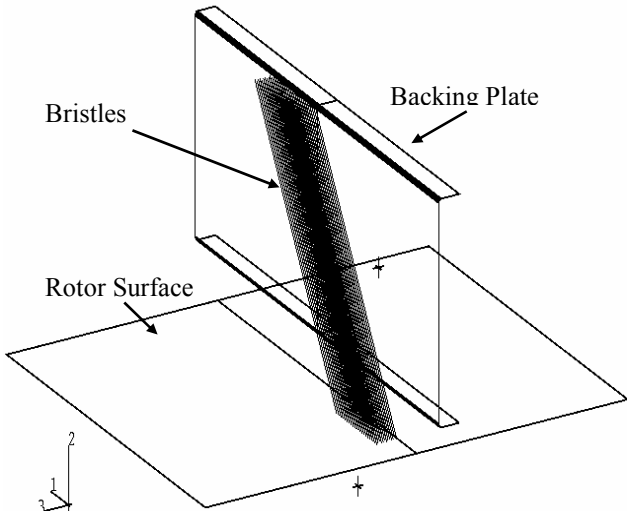

Fig. 2 The 3-D finite element model of a brush segment.

FINITE ELEMENT MODEL

During operation, bristles experience deflection in a radial plane due to rotor excursion, while they bend axially under pressure load. Therefore, a three-dimensional solution is required for a proper brush seal analysis. The model consists of a representative bristle bundle with a backing plate and a rotor surface (Fig. 2). Every bristle is defined by a number of 3-D quadratic beam elements. The rotor and the backing plate are defined as rigid surfaces. A representative backing plate is placed behind the first bristle row of bristles. In addition to the main design parameters defined in Fig. 1, analysis requires information on material properties, bristle diameter and friction coefficients for various contact locations.

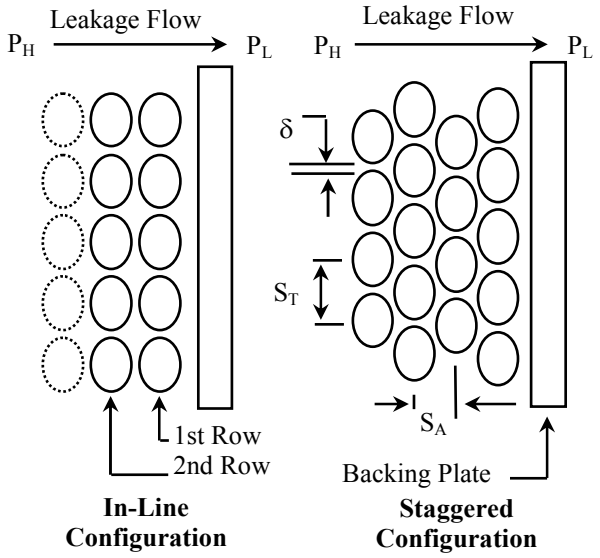

Fig. 3 Possible bristle layouts in circumferential plane.

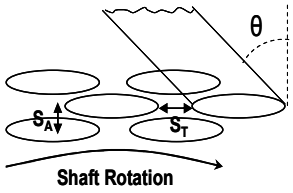

Fig. 4 Footprints of bristles on the shaft surface.

Modeling of bristle spacing involves layout and proximity. Within the brush pack two types of bristle layouts can be considered in the circumferential plane, namely, in-line or staggered (Figs. 3 and 4). The actual spacing will be a mixture of these two. Microscopic inspections reveal that in a typical seal most of the bristles tend to stay in a staggered configuration. Therefore, the presented analysis incorporates the staggered configuration to achieve a better simulation of the real case. As manufacturing aims for the highest attainable density, bristle spacing usually gets close to the minimum geometrically possible. Crudgington et al [1] reported 15% blooming in thickness at free state. However, current model considers 25% blooming for the axial spacing, S_A. Extra axial space helps reduce solver problems in the initial phase of the analysis. These values define initial spacing for the presented model where bristles immediately compact upon application of pressure load. Since there is no coupled CFD analysis, applied aerodynamic loading does not change with spacing. On the other hand, spacing is extremely important for brush seal leakage and flow models.

As for the tangential spacing (S_T), the analysis defines 5% of the minimum geometric center-center distance as the gap (δ) to represent common seal density of ~2000 bristles per inch of rotor circumference.

Depending on the bristle diameter a standard density brush seal can have 8-12 bristle rows in rotor axial direction. The model has been successfully tested up to 20 bristles in a row, and up to 16 bristles rows without any convergence or numerical stability problems. This allows simulation capability from standard to double density seal designs.

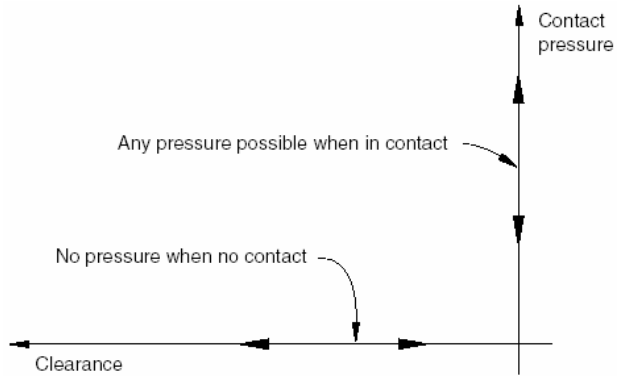

Fig. 5 Pressure-clearance relationship for bristle-rotor contact surface pairs.

Contact Definitions

Based on the physical nature of the interactions, three types of contacts are modeled. The interaction between the bristle tips and the rotor is defined as a rigid surface contact where rotor is infinitely rigid while bristles are allowed to deform. In this interaction, contact loads are transmitted as soon as the tip node of a bristle touches the rotor surface. Since the rotor is defined as the rigid surface, it represents the master surface in the bristle-rotor contact pairs. The first two or three beam elements at the tip of each bristle are defined as stress-displacement rigid surface elements which are coupled with the rotor surface. These elements represent the slave surface. They are allowed to be compliant and deformable. The nodes of the slave surface can not penetrate into the master surface. Therefore, contact direction is always normal to the master surface. For bristle-rotor contacts, pressure-clearance relationship is defined as illustrated in Fig. 5. This allows contact pressure to build-up only after the tip node of a bristle touches the rotor.

The interaction between the first row of bristles and the backing plate is similar to that of the rotor contact. However, contact is detected when bristle center nodes are at a distance of bristle radius away from the backing plate (see Fig. 6). This type of pressure-clearance relationship is called softened contact. Inter-bristle interactions involve deformation of both of

the bodies. Therefore, they are modeled using slide lines. In a slide line contact, elements of one of the interacting bodies slide against the line defined by the nodes of the other body. This line of interaction is defined by attaching slide line contact elements to the surface of one of the bodies, and associating these elements with a set of nodes on the other surface. Fig. 7 illustrates the slide line concept. Relative motion along the line of interaction can be arbitrarily large. But relative motions out of the plane containing the line of interaction are assumed to be comparably small.

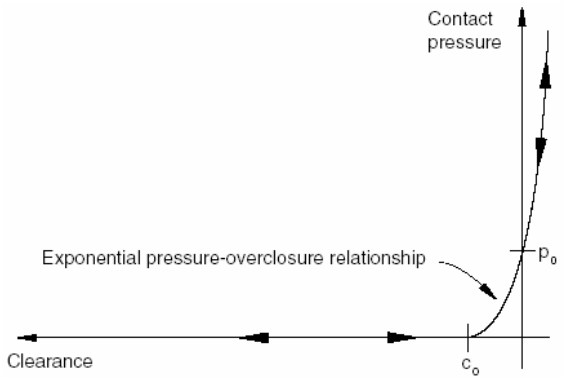

Fig. 6 "Soft Contact" pressure-clearance relationship for bristle-backing plate and bristle-bristle contact surface pairs.

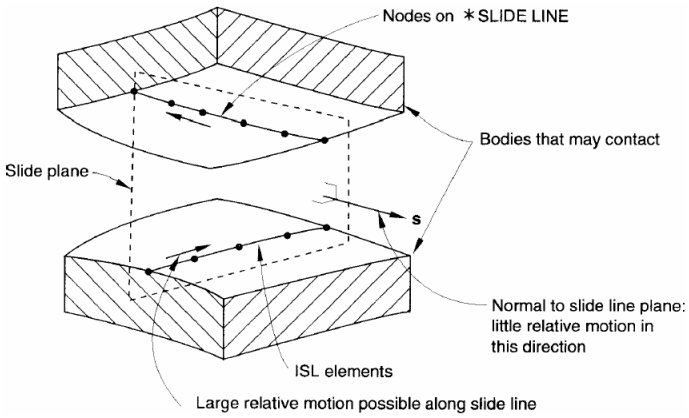

Fig. 7 Slide line concept in a contact pair.

If the interacting bodies are cylinders/tubes, as the case here, through the use of special slide line contact elements, the relative motion is allowed to be along a curve of contact. In this case, the contact direction is normal to the slide line in the direction of the smallest distance between the surfaces of the cylinders (bristles). For a bristle couple, all the nodes in one of the bristles form the slide line. The corresponding second order slide line contact elements on the other bristle are defined. Fig. 8. illustrates the use of slide lines between the bristles. The model does not include the first node at the free tip in the contact elements to avoid over constraining the tip node as it is also in contact with the rotor surface. The last two nodes at the top of the bristles are also spared, as they would be over constrained. Bristles are fixed at this end, and these nodes will not see any sizable sliding. The contact is detected at a bristle diameter distance between the two node-sets located at the bristle centerlines. Both inter-bristle and backing plate contacts incorporate additional surface roughness involved when calculating contact detection distances.

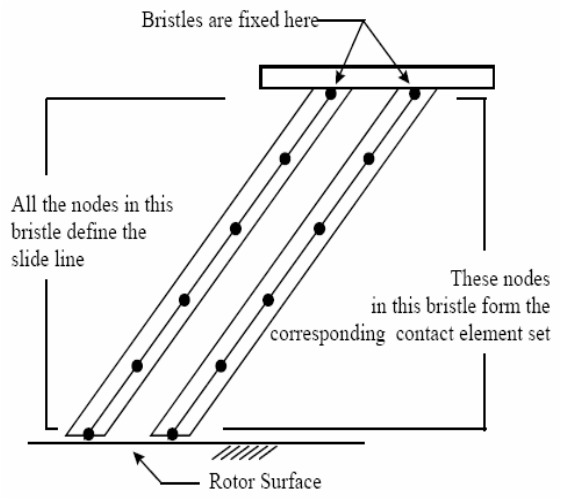

Fig. 8 Application of slide lines in a bristle pair.

Friction Modeling

The analysis incorporates classical isotropic coulomb friction model for all contacts. When two bodies are in-contact both shear and normal forces are transmitted across the interface. The incorporated coulomb friction model assumes that no relative motion occurs until the equivalent frictional shear stress reaches a threshold value which depends on the friction coefficient defined for that contact. The critical stress, τ_{crit}, is proportional to the contact pressure, p, in the form

$$\tau_{crit} = \mu p$$

where μ is the friction coefficient (Fig. 9). This standard isotropic constant friction model facilitates an easier solution to the complicated frictional contact problems. The reported values of friction coefficient for common Haynes 25 fiber widely vary from 0.08 to 0.47 under different test conditions. Crudgington et al [1] obtained steady readings of 0.28 when running against stainless steel. This value is taken as an average overall friction coefficient in the presented analysis.

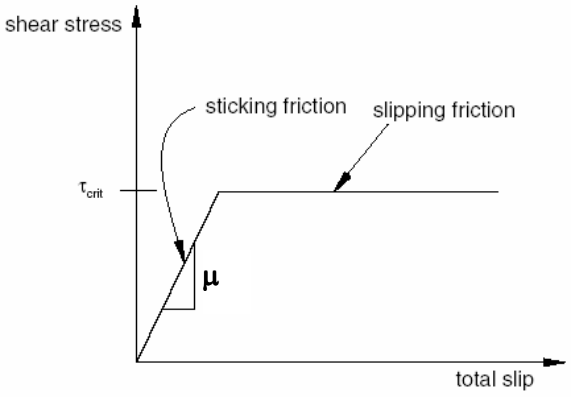

Fig. 9 Friction model used in the analysis.

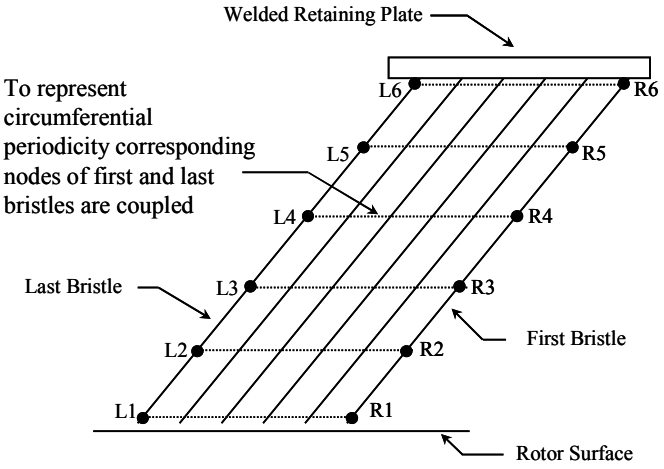

Fig. 10 Coupling of end bristle nodes in a row in the analysis.

Boundary Conditions

Proper application of the boundary conditions is necessary for an accurate analysis. Due to the strong pressure-friction coupling present in brush seals, loading sequence is critical. If pressure is applied after a prescribed radial interference, the contact loads will be lower than the case where a pressure is applied before the rotor interference. Most real applications involve the latter case. The analysis updates pressure load distribution at every displacement increment as radial locations of elements change during rotor interference.

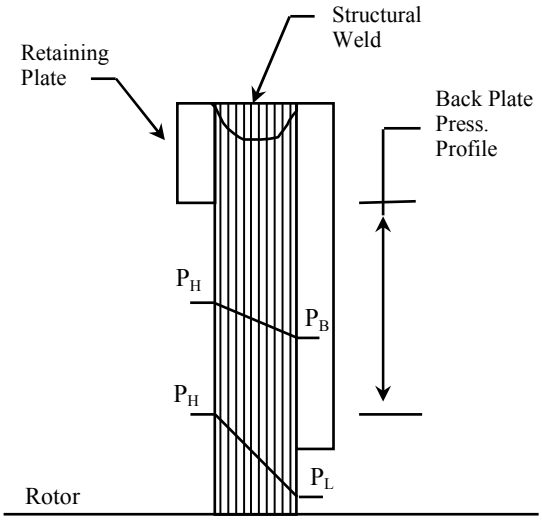

Fig. 11 Pressure boundary conditions.

To represent bristle clamping and the weld at the periphery, all 6 degrees of freedom (both translations and rotations) for top node of each bristle is constrained. Frictional contact defined at backing plate limits axial bristle motion. Bristles are free to slide on the backing plate or to bend below the fence height under axial pressure load. Frictional contact defined at bristle tips allows bristles to slide tangentially, or to bend axially when rotor surface is moved towards the brush pack under pressure. To provide circumferential periodicity, first and last bristles in each row are coupled in a master-slave relationship (Fig. 10). The last bristle at every row experiences a pull from the first, instead of the resistance from the rest of the bristles behind it. Similarly, this load transfer allows the first bristle to experience a pull from the last bristle rather than a push by the rest of the bristles before it. Seal-rotor interference is simulated by applying radial displacements to the rigid body node representing the rotor surface. Rotor surface can also be assigned circumferential velocity to simulate actual rotor rotation in service.

Pressure distribution in and around the bristle pack defines the axial and radial pressure loads on each bristle. For accurate pressure boundary condition both axial and radial pressure profiles are needed. Measurements by Bayley et al [2] and observations by Braun et al. [3] suggest almost a linear axial pressure drop. Therefore, the model incorporates a linear axial pressure drop within the bristle pack as illustrated in Fig. 11. An arbitrary bristle in the middle of the pack is loaded by a prescribed axial force due to leakage flow (axial pressure drop) while it is also subjected to the contact forces transmitted by the adjacent bristles. Axial pressure difference across the bristle pack varies with the radial position along the backing plate while portion of the seal at the fence height region experience the maximum pressure load. Radial pressure profile can be estimated by pressure variation along the backing plate. Pressure at the backing plate (P_B) is close to upstream pressure (P_H). It quickly drops to downstream pressure (P_L) near the inner edge of the backing plate. The model uses a radial pressure profile based on the data provided by Bayley et al. [2] and Turner et al. [4].

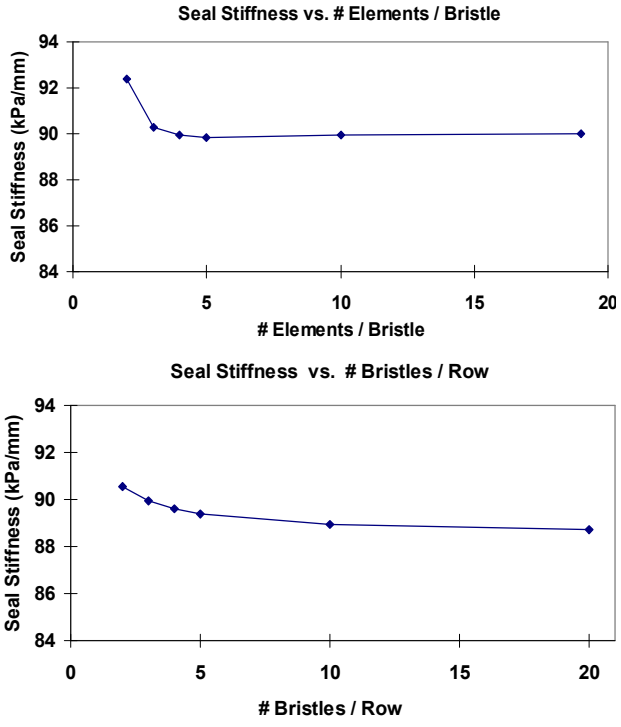

Fig. 12 Mesh sensitivity analyses.

Using a FORTRAN code, problem is defined, and the 3-D model is generated based on design parameters and boundary

conditions. Once the model is ready, ABAQUS solver routines are utilized to obtain stress and displacement solutions. The model results are tested for mesh sensitivity. Five quadratic elements per bristle, and 4-5 bristles per row are identified as optimal mesh numbers (Fig. 12). This also translates to 3-4 hours solution time for a typical 10-13 row brush seal on an SGI Origin 2000 machine. Although the model allows for up to 99 bristle rows with 100 bristles in each, solution time increases exponentially and convergence problems arise as mesh size gets larger.

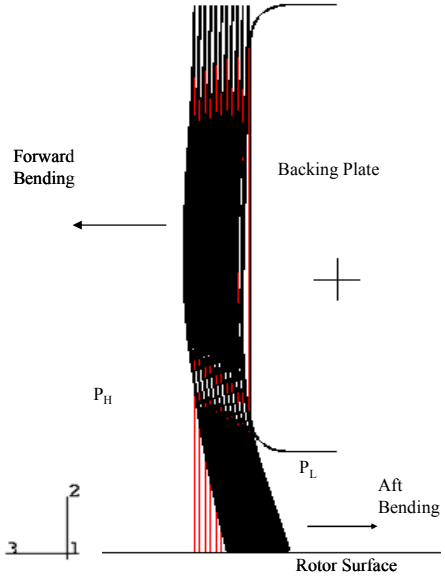

A) Pressure application

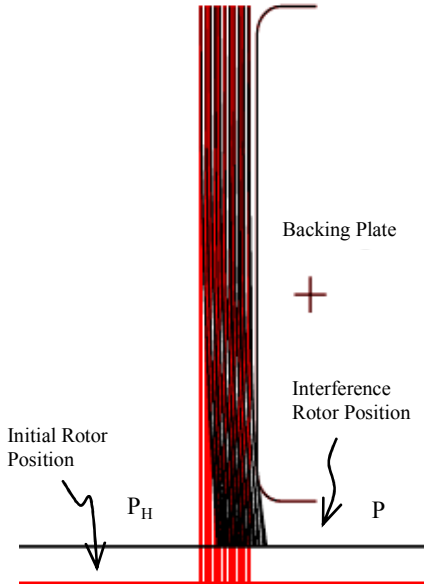

B) Application of rotor interference under pressure load.

Fig. 13 Seal deflection under combined pressure and interference loading. (Red indicates starting mesh)

RESULTS AND DISCUSSION

Once ready, the model is tested for both pressure and interference load cases. As illustrated in Fig.13, analysis accurately models 3-D seal behavior under pressure load. When rotor interference is removed under pressure, analysis can accurately predict seal hysteresis as illustrated in Fig. 14. The model has been further verified through stiffness and wear tests. A 31.267 mm (1.231 in.) seal segment (having 3016 fibers) is cut from a 101.6 mm (4 in.) bore brush seal. Seal design variables used in wear tests are tabulated in Table 1. Bristles are made of Haynes-25 material, while 101.6 mm (4 in.) diameter test rotor is made from 410 stainless steel with a 0.41 μm (16 μin.) surface finish.

Table 1 Design parameters for test seals and analyses.

	Parameter	Value	
Bristle Diameter	d	0.071 mm	0.0028 in
Free Bristle Height	BH	6.833 mm	0.269 in
Fence Height	FH	1.4 mm	0.055 in
Cant Angle	θ	45 deg	45 deg
Bristle Density	η	97 /mm	2450 /in
Rotor Radius	R	50.8 mm	2 in

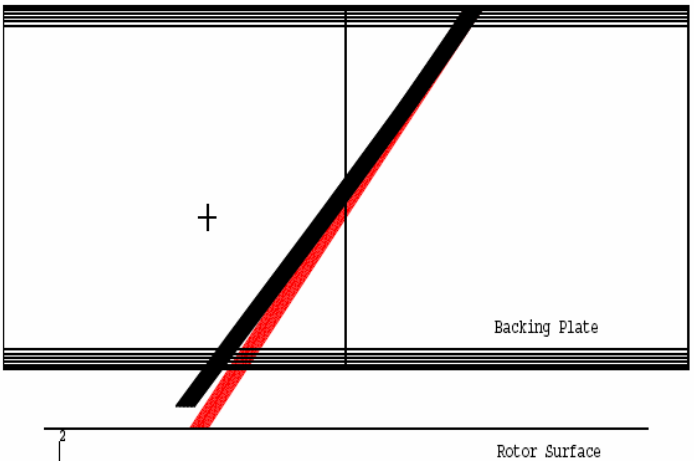

Fig. 14 Simulation of seal hang-up/hysteresis.

First, shining light from far side, line-to-line condition is established through a magnifying glass. From this baseline level, the seal is pushed towards rotor, and locked at 0.762 mm (0.030 in.) radial interference position. Radial displacements are verified through a fine graduation dial indicator. Wear tests are conducted at room temperature with 29 m/s (96 ft/s) surface speed under constant prescribed radial interference for a total of 6 hours. To capture the initial wear-in phase, weight measurements are taken in the first 15 minutes and 30 minutes. After the first hour, measurements are taken at one hour intervals. In order to compare test results with analysis, wear volumes corresponding to each time interval are calculated.

Dimensional wear coefficient is defined by

$$K = \frac{V_L}{F_n S_D}$$

where V_L is the wear volume lost, F_n is the normal load for the test piece, and S_D is the distance slid. Rearranging this relation will yield the wear volume as

$$V_L = K F_n S_D.$$

Once bristle-rotor contact force is obtained from the analysis, wear volume can be calculated. Based on Fellenstein et al.s [5] room temperature measurements, wear coefficient is taken as $K=1.2x10^{-6}$ mm^3/Nm for the calculation of room temperature wear tests. Multiplying wear volumes by the bristle material density of 9.13 gr/cm^3 yields estimated lost mass. Analytical and experimental wear results are compared in Fig.15. The analytical results show a good match for the measurements at the start of the tests. After the initial wear-in, with gradual loss of interference, experimental wear rate starts decreasing, and the difference increases. This behavior is expected as analysis is performed for a prescribed interference load. However, it should be taken one step further for an iterative solution where radial interference will be reduced as wear progresses.

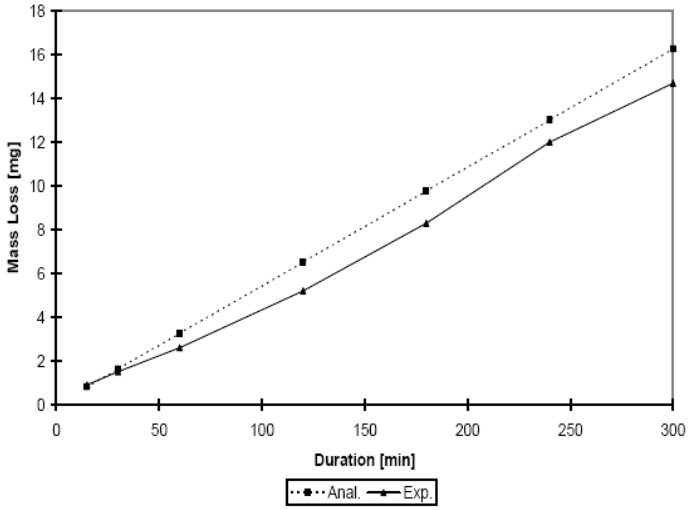

Fig. 15 Comparison of model wear predictions with test results for 29 m/s test.

As a final stage of verification, model has been tested for blow-down/pressure-closure behavior. First, rotor surface has been moved away from the brush. Then, pressure load introduced and gradually increased. As illustrated in Fig. 16, results indicate that model can accurately predict closure of bristles towards rotor with increasing pressure load. Overall, the 3-D finite element model effectively captures physical seal behavior.

REFERENCES

[1] Crudgington, P. F, and Bowsher, A., "Brush Seal Pack Hysteresis," (2002) AIAA Paper No. AIAA-2002-3794.

[2] Bayley, F. J., and Long, C. A., "A Combined Experimental and Theoretical Study of Flow and Pressure Distributions in a Brush Seal," ASME J. Eng. Gas Turbines Power, 115, No. 2, (1993) 404-410.

[3] Braun, M. J., Hendricks, R. C., and Canacci,V., "Flow Visualization in a Simulated Brush Seals," (1990) ASME Paper No. 90-GT-217.

[4] Turner, M. T., Chew, J. W., and Long, C. A., "Experimental Investigation and Mathematical Modeling of Clearance Brush Seals," ASME J. Eng. Gas Turbines Power, 120, No. 3, (1998) 573-579.

[5] Fellenstein, J.A. and Dellacorte, C., 'A New Tribological Test for Candidate Brush Seal Materials Evaluation,' Trib. Trans., 39, (1996) 173-179.

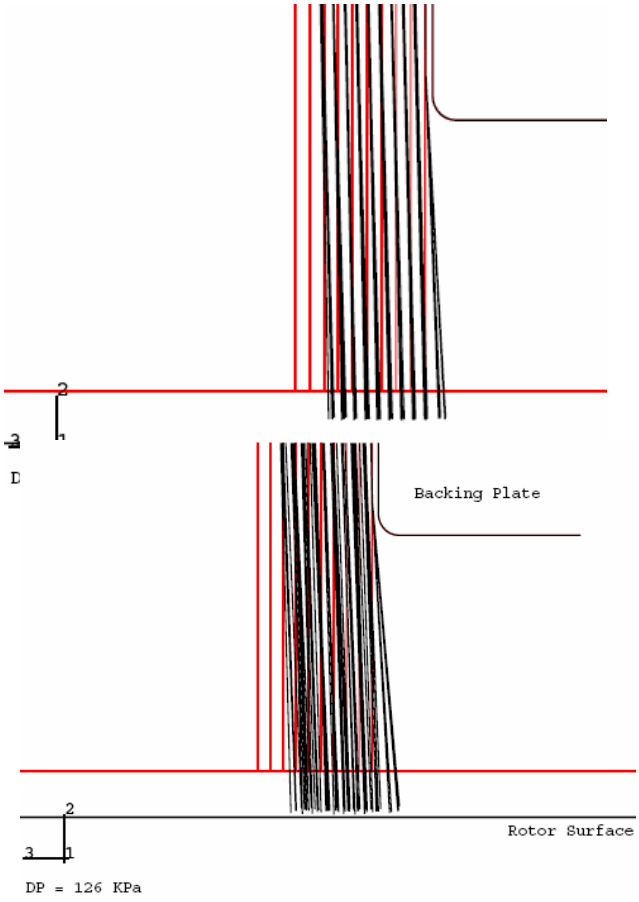

B) 126 kPa pressure load.

Fig. 16 Analysis pressure closure. First rotor is moved away from the seal, than pressure load is increased in two levels. (Red indicates starting mesh)